Articles

tRNA−Guanine Transglycosylase from *Escherichia coli*: Molecular Mechanism and Role of Aspartate 89†

Jeffrey D. Kittendorf, Lisa M. Barcomb, Susanne T. Nonekowski, and George A. Garcia*

Department of Medicinal Chemistry, College of Pharmacy, University of Michigan, Ann Arbor, Michigan 48109-1065

Received May 22, 2001; Revised Manuscript Received September 28, 2001

ABSTRACT: The enzyme tRNA−guanine transglycosylase (TGT, EC 2.4.2.29) catalyzes a posttranscriptional transglycosylation reaction involved in the incorporation of the modified base queuine [Q, 7-(4,5-*cis*-dihydroxy-2-cyclopenten-1-ylaminomethyl)-7-deazaguanine] into tRNA. Previously, the crystal structure of the TGT from *Zymomonas mobilis* was solved in complex with preQ$_1$ (the substrate for the eubacterial TGT) [Romier et al. (1996) *EMBO J. 15*, 2850−2857]. An aspartate residue at position 102 (position 89 in the *Escherichia coli* TGT) was proposed to play a nucleophilic role in an associative catalytic mechanism. Although this is an attractive and precedented mechanism, a dissociative mechanism is equally plausible. In a dissociative mechanism, aspartate 89 would provide electrostatic stabilization of an oxocarbenium ion intermediate that is formed by dissociation of guanine. To clarify the nature of the catalytic mechanism of TGT, we have generated and characterized four mutations of aspartate 89 in the *E. coli* TGT (alanine, asparagine, cysteine, and glutamate). All four mutant TGTs were able to noncovalently bind tRNA, but only the glutamate mutant was able to form a stable complex with the RNA substrate under denaturing conditions that was comparable to wild type. Furthermore, the glutamate mutant was the only mutant TGT that demonstrated significant activity. Kinetic parameters were determined for this enzyme and shown to be comparable to wild type, revealing that the enzyme is considerably tolerant of the positioning of the carboxylate. Under conditions of high enzyme concentrations and long time courses, the alanine, asparagine, and cysteine mutants showed very low levels (ca. 10^3-fold lower than wild type) of activity that were linear with respect to enzyme concentration and dependent upon pH in a fashion similar to that of the wild type. However, the observed initial velocities were too low to accurately determine k_{cat} and K_m values. We hypothesize that the activity observed for these mutants is most likely derived from host strain TGT (wt) contamination. These results are most consistent with aspartate 89 acting as a nucleophile in an associative catalytic mechanism.

tRNA−guanine transglycosylase (TGT, EC 2.4.2.29) is a key enzyme involved in the posttranscriptional modification of tRNA across the three domains of life. TGT[1] catalyzes a base-exchange reaction that involves the cleavage of a guanosine *N*-ribosyl bond without breakage of the phosphodiester backbone. In both eubacteria and eukaryotes, with the exception of yeast, TGT activity ultimately leads to modification of tRNAs with the hypermodified base queuine [7-(4,5-*cis*-dihydroxy-1-cyclopenten-3-ylaminomethyl)-7-deazaguanine, Figure 1]. In contrast, the TGT from archaebacteria yields tRNA modified with the closely related base archaeosine (7-formamidino-7-deazaguanine, Figure 1).

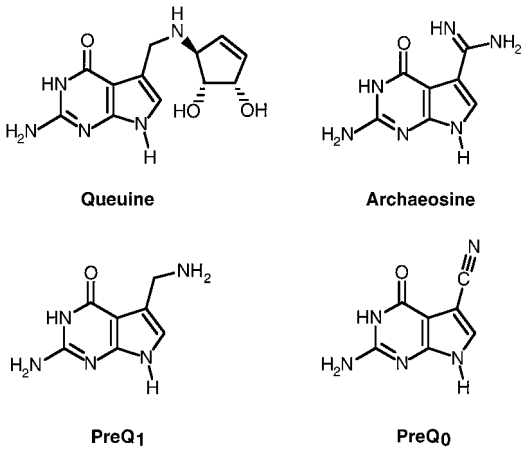

FIGURE 1: Structures of queuine, archaeosine, preQ$_1$, and preQ$_0$.

† This work was supported in part by the National Science Foundation (MCB9720139 to G.A.G.), the National Institutes of Health (GM07767 to J.D.K., trainee), and the University of Michigan, College of Pharmacy, Vahlteich Research Fund.

* To whom correspondence should be addressed. Phone: (734) 764-2202. Fax: (734) 763-5633. E-mail: gagarcia@umich.edu.

[1] Abbreviations: TGT, tRNA−guanine transglycosylase; IPTG, isopropyl β-D-thiogalactopyranoside; DTT, dithiothreitiol; HEPES, *N*-(2-hydroxyethyl)piperazine-*N*′-2-ethanesulfonate; Tris·HCl, tris(hydroxymethyl)aminomethane hydrochloride; PMSF, phenylmethanesulfonyl fluoride; SDS, sodium dodecyl sulfate; PAGE, polyacrylamide gel electrophoresis; TCA, trichloroacetic acid; htTGT (wt), histidine-tagged wild-type TGT. Histidine-tagged TGT mutant enzymes are referred to according to the following pattern: htTGT (D89A) (i.e., aspartate 89 mutated to alanine).

10.1021/bi0110589 CCC: $20.00
Published on Web 11/02/2001

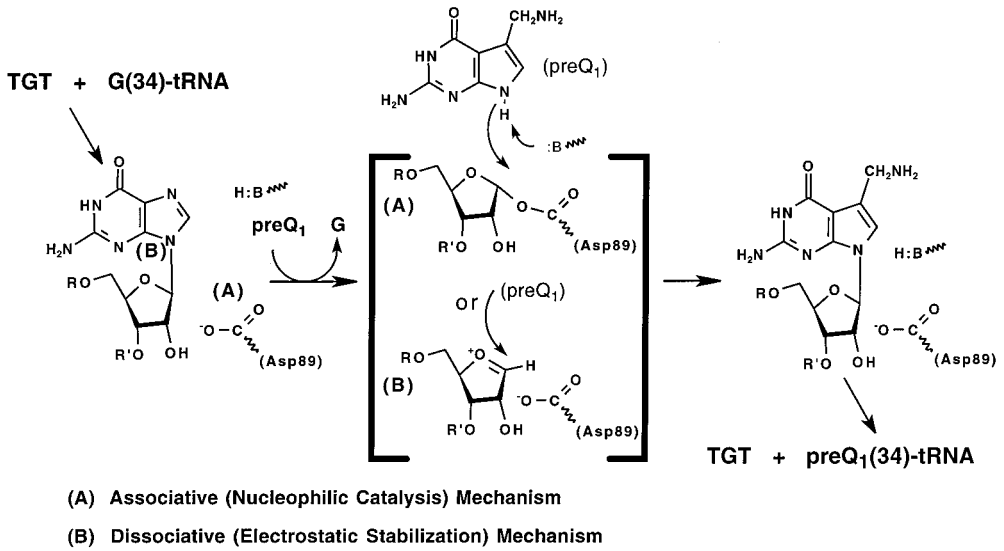

FIGURE 2: Proposed catalytic mechanisms of tRNA−guanine transglycosylase.

Despite the significant levels of sequence similarity (~40%) among the TGTs from the three domains, differences exist in the substrate specificity of the tRNA and/or the heterocyclic base. In eubacteria, TGT catalyzes the exchange of a queuine precursor ($preQ_1$, 7-aminomethyl-7-deazaguanine, Figure 1) for the guanine found in the wobble position (position 34) of tRNAs that have an anticodon sequence of GUN (Asp, Asn, His, and Tyr). Once incorporated into tRNA, $preQ_1$ undergoes further chemical transformation through at least two subsequent enzymatic steps to yield the final queuine modification (*1*, *2*). In contrast, the eukaryotic TGT directly incorporates queuine into position 34 of cognate tRNAs. In higher organisms, queuine is further modified by glycosylation of the cyclopentene diol with either mannose or galactose (*3*). The archaebacterial TGT differs from the previous two in both heterocyclic substrate and tRNA substrate. This TGT catalyzes the base-exchange reaction of $preQ_0$ (7-cyano-7-deazaguanine, Figure 1) for a guanine found at position 15 in the D-loop of archaeal tRNAs (*4*, *5*). The $preQ_0$ is then presumably converted to archaeosine via an uncharacterized chemical transformation.

Much work has been done to characterize the eubacterial TGT. Studies using the TGT from *Escherichia coli* have resulted in an understanding of the gross structural characteristics of the eubacterial TGTs as well as their substrate recognition properties with regard to both the tRNA (*6*−*11*) and the heterocyclic base (*12*). The crystal structure of the *Zymomonas mobilis* TGT was solved at 1.85 Å, revealing a noncanonical $(B/\alpha)_8$ -barrel fold (*13*). Soaking of the crystals with the heterocyclic substrate $preQ_1$ allowed identification of the active site, which is located at the C-terminal face of the barrel (*14*). On the basis of this structure, it was suggested that aspartate 102 (aspartate 89, *E. coli* numbering) was positioned to play an important role in TGT catalysis. Interestingly, despite the substrate differences found across the three TGT classes, this residue is invariant in all TGT sequences known to date. Romier et al. have demonstrated that replacement of aspartate 102 with alanine leads to complete loss of enzymatic activity; furthermore, this mutant is unable to form a "covalent complex" with substrate tRNA as judged by SDS−PAGE (*15*). Consequently, it was proposed that aspartate 102 was acting as an enzymic nucleophile in a double displacement catalytic mechanism whereby its attack of the 1′-carbon of the ribose leads to displacement of the guanine base (Figure 2).

A similar associative mechanism has been previously reported for other enzymes involved in cleavage of glycosidic bonds. 2′-Deoxyribosyltransferase catalyzes the glycosidic bond cleavage of 2′-deoxyribonucleosides. A glutamate residue has been identified to be the active site nucleophile of this enzyme (*16*, *17*). Likewise, "retaining glycosyl hydrolases" catalyze the hydrolysis of glycosidic bonds with retention of configuration. These enzymes utilize the carboxylate moiety from either glutamate (*18*−*21*) or aspartate (*22*, *23*) as the active site nucleophile. A second active site carboxylate functions as a general acid/base by donating a proton to the leaving group and then abstracting a proton from the incoming water. Furthermore, a conserved aspartate in pseudouridine synthase that is essential for activity has been proposed to act as a nucleophilic catalyst, attacking the 1′-carbon of the ribose moiety (*24*).

The observation of a covalent complex between tRNA and TGT is not sufficient to prove that this intermediate is on the normal reaction pathway. A dissociative catalytic mechanism can also be proposed for TGT catalysis whereby the aspartate residue provides electrostatic stabilization of an oxocarbenium ion transition state (Figure 2). Precedent for this type of mechanism is found in the nucleoside hydrolases. Like TGT, these enzymes facilitate cleavage of C−N glycosidic bonds. The transition states of the nucleoside hydrolases are characterized by protonation of the heterocyclic leaving group and extensive oxocarbenium ion character that is developed by the flattening of the ribofuranosyl ring (*25*, *26*). The nonbonding electrons of the incoming water are proposed to stabilize the positive charge. In the case of TGT, this role could be fulfilled by the carboxylate of aspartate 89.

It is equally possible that catalysis by TGT could be achieved through either an associative or a dissociative mechanism. Therefore, to distinguish between these two differing mechanisms and to gain a better understanding of the role of this active site aspartate, we initiated a more comprehensive mutagenesis study whereby aspartate 89 of the *E. coli* TGT was mutated to alanine, asparagine, cysteine,

Table 1: Primers Used for Site-Directed Mutagenesis[a]

Mutagenic Primer	Sequence (5' to 3')
WT	G GGG CCG ATC CTC ACC **GAC** TCC GGC GGC TTC CAG G
D89A[1]	G GGG CCG ATC CTC ACG **GCC** TCA GGC GGC TTC CAG G
D89C[2]	G GGG CCG ATC CTC ACG **TGC** TCA GGC GGC TTC CAG G
D89E[3]	G GGG CCG ATC CTC ACT **GAG** TCC GGC GGC TTC CAG G
D89N[4]	G GGG CCG ATC CTC ACG **AAT** TCC GGC GGC TTC CAG G

[a] Complementary primers were used for QuikChange mutagenesis. D89 and mutations are designated in bold. Restriction sites ([1]*Bsu*36I, [2]*Pml*I, [3]*Dde*I, [4]*Eco*RI) used for screening are underlined.

and glutamate. The results of the biochemical characterization of these four mutants are most consistent with an associative (nucleophilic) mechanism for TGT catalysis.

MATERIALS AND METHODS

Reagents. Unless otherwise specified, chemical reagents were purchased from either Sigma or Aldrich. Agarose, isopropyl β-D-thiogalactopyranoside (IPTG), and dithiothreitol (DTT) were from Gibco BRL. SeaPlaque low melting point agarose was from FMC BioProducts. Tris·HCl buffer was from Research Organics, and HEPES was from United States Biochemical. Restriction enzymes and Vent DNA polymerase were from New England Biolabs. Gelase agarose digesting enzyme was from Epicenter. T4 DNA ligase, kanamycin, and chloramphenicol were from Boehringer Mannheim. Plasmid pTGT5 was from a laboratory stock (*27*), and plasmid pET28a was from Novagen. Epicurian Coli XL2-Blue ultracompetent cells were from Stratagene, TG2 cells were from a laboratory stock, and BL21(DE3) pLysS cells were from Novagen. Bradford reagent was from Bio-Rad. His·Bind resin was from Novagen. The *E. coli* tyrosyl tRNA (ECY) transcript was prepared as described previously (*10*). [8-^{3}H]Guanine (5−15 Ci/mmol) and [8-^{14}C]guanine (50−60 mCi/mmol) were from Moravek. [8-^{14}C]Guanine$_{34}$-labeled tRNA (2.15 mCi/mmol) was prepared as described previously (*12*). DNA oligonucleotides for mutagenesis (Table 1) were synthesized at the University of Michigan, Biomedical Research Core Facility (UM-BRCF).

Construction of Aspartate 89 TGT Mutants. Mutants of aspartate 89 were generated from the wild-type *E. coli* TGT expression plasmid (pTGT5) using QuikChange site-directed mutagenesis (Stratagene). Briefly, 10 μL reactions containing 800 ng of plasmid pTGT5, 150 ng each of the respective mutagenic primers, and 3 units of Vent DNA polymerase were subjected to 15 PCR cycles of the following temperature sequence: 94 °C for 1 min, 50 °C for 1 min, and 72 °C for 5.5 min. Following digestion with 20 units of *Dpn*I for 1 h, 10 μL of the PCR product was transformed into 100 μL of ultracompetent Epicurian Coli XL2-Blue cells according to vendor's protocols. The transformed cells were spread on L-agar plates containing 50 μg/mL ampicillin. Harvested plasmid DNA was screened for the desired mutation by restriction digestion with the enzymes noted in Table 1. DNA sequencing (UM-BRCF) was used to verify the absence of undesired mutations in each of the *tgt* mutant genes. The mutant plasmids were designated pD89A (alanine), pD89C (cysteine), pD89E (glutamate), and pD89N (asparagine).

Generation of the Amino-Terminal His-Tag TGT Mutant Constructs. Mutant *tgt* genes were excised from pD89A, pD89C, pD89E, and pD89N by double digestion with *Nde*I and *Hin*dIII. The *tgt*-containing *Nde*I/*Hin*dIII fragments were separated from the parent plasmids on 1% SeaPlaque agarose by gel electrophoresis. The bands corresponding to the mutant *tgt* genes were excised from the gel and were treated with one unit each of Gelase agarose digesting enzyme. Each of the *tgt*/*Nde*I/*Hin*dIII fragments (8 μL) and similarly treated pET28a (2 μL) were ligated in 20 μL reaction mixtures containing 2 units of T4 DNA ligase. The ligation reactions were performed at 16 °C for 16 h. Each ligation reaction (3 μL) was used to transform 150 μL of competent *E. coli* TG2 cells. The transformation reactions were incubated on ice for 30 min and then were heat shocked at 42 °C for 90 s. The transformed cells were spread on L-agar plates containing 30 μg/mL kanamycin. Plasmids were isolated from a maximum of five colonies per plate. Restriction digests (as previously mentioned, Table 1) were used to verify the presence of the mutant *tgt* genes. The plasmids were named pHD89A (alanine), pHD89C (cysteine), pHD89E (glutamate), and pHD89N (asparagine).

Expression and Purification of Aspartate 89 TGT Mutants. pHD89A, pHD89C, pHD89E, and pHD89N (2 μL each) were transformed into 150 μL of competent *E. coli* BL21-(DE3) pLysS, and the transformed cells were spread on L-agar plates containing 30 μg/mL each of kanamycin and chloramphenicol. One colony per mutant was used to inoculate 3 mL of 2×TY media containing 30 μg/mL kanamycin and 30 μg/mL chloramphenicol. The cultures were grown overnight at 37 °C with shaking.

Overnight cultures (500 μL each) were used to inoculate 500 mL of fresh 2×TY containing the appropriate concentration of kanamycin and chloramphenicol. The cultures were incubated at 37 °C with vigorous shaking until the OD_{600} reached ∼0.60. Mutant TGT expression was induced by the addition of IPTG to each culture to a final concentration of 1 mM. The cultures were allowed to incubate an additional 2 h postinduction, after which time the cells were harvested by centrifugation (4500*g*, 15 min, 4 °C).

All purification steps were performed at 4 °C. The cell pellets from the 500 mL cultures (∼1.4−1.6 g wet weight) were resuspended in 15 mL of lysis buffer (20 mM Tris·HCl, pH 7.9, 500 mM NaCl, 5 mM imidazole, 100 μM PMSF). The cellular suspensions were incubated on ice for 30 min to allow for lysis by the pLysS-encoded T4 lysozyme, after which time the cellular debris was pelleted by ultracentrifugation (100000*g*, 1 h, 4 °C). The supernatant was sterile filtered with a 0.22 μm syringe filter (Millipore) and applied to a column packed with nickel-charged His·Bind resin that had been equilibrated with 6 mL of lysis buffer. Following the loading of the supernatant, the column was washed with 20 mL of lysis buffer, followed by 15 mL of wash buffer (20 mM Tris·HCl, pH 7.9, 500 mM NaCl, 60 mM imidazole). The amino-terminal His-tagged TGTs were eluted from the column with 15 mL of elution buffer (20 mM Tris·HCl, pH 7.9, 500 mM NaCl, 350 mM imidazole) and collected in 1 mL fractions. EDTA was added to each fraction (10 mM final concentration) in order to chelate any nickel that may have leeched from the column.

Fractions containing the mutant enzymes of interest were identified by the presence of a 44 kDa band on SDS−PAGE. The fractions were pooled and subjected to 15 h dialysis against 25 mM HEPES, pH 7.3, 2 mM DTT, 1 mM EDTA, and 100 μM PMSF. Immediately following the initial 15 h dialysis, the enzyme fractions were dialyzed for 24 h against two changes of equilibration buffer (25 mM HEPES, pH 7.3, 2 mM DTT, 100 μM PMSF). Enzymes were concentrated using ultrafiltration spin columns (BioMax 10 K, Millipore). The final concentration of each mutant TGT was determined with the Bio-rad protein assay kit based on the Bradford method using BSA standards. The TGT mutants, hereafter referred to as htTGT (D89A), htTGT (D89C), htTGT (D89E), and htTGT (D89N), were stored in liquid nitrogen until needed.

tRNA Binding: Native PAGE. To assess the noncovalent binding of the *E. coli* tyrosyl-tRNA (ECY) substrate to the mutant TGTs, native PAGE band-shift assays were performed as previously described *(7, 8)*. Briefly, 3 μM TGT was incubated with a 10-fold excess of ECY at 37 °C for 1 h in a reaction mixture containing 10 mM HEPES, pH 7.3, 1 mM $MgCl_2$, and 10 mM DTT. The reaction mixtures were then analyzed by native PAGE using 8−25% gradient polyacrylamide gels (Pharmacia). Approximately 4 μL of each reaction was loaded on the gel and run under native conditions following the vendor's protocols. Following electrophoresis, the gels were first stained by ethidium bromide for tRNA visualization and then by Coomassie blue for protein visualization.

Denaturing PAGE: Covalent Complex Band-Shift Assay. The abilities of htTGT (wt) and htTGT (mutants) to form a stable complex with tRNA were assessed by a denaturing PAGE band-shift assay. Enzyme (5 μM) was incubated with a 4-fold excess of dG_{34}-ECYMH (20 μM), a minihelical analogue of ECY consisting of the anticodon stem and loop substituted with a deoxyguanosine located at position 34, in the presence of 400 μM 9-methylguanine at 37 °C for 1 h in a 10 μL reaction mixture containing 10 mM HEPES, pH 7.3, and 1 mM $MgCl_2$. SDS buffer (10 μL, 60 mM Tris·HCl, pH 6.8, 2% SDS, 10% glycerol, 0.01% bromophenol blue) was added to the reaction mixtures, and the incubation was continued at room temperature for an additional 1 h. Aliquots (4 μL) of each reaction were loaded onto a gradient 8−25% polyacrylamide gel and run under denaturing conditions following the vendor's protocols (Pharmacia). The gel was stained with Coomassie blue to visualize the protein.

Activity Screen. A previously described guanine-exchange assay (TGT assay) was used to assess the activity of each of the aspartate 89 TGT mutants with slight modifications *(8, 11)*. Enzyme (250 nM−2 μM final concentration) was introduced to a 550 μL reaction mixture of 100 mM HEPES (pH 7.3), 5 mM DTT, and 20 mM $MgCl_2$ containing 20 μM ECY tRNA and 20 μM [8-^{14}C]guanine (39.8 mCi/mmol). The reaction progress was monitored over a time course of 4 h. Aliquots (70 μL) of each reaction mixture were withdrawn at designated time points, quenched in 2 mL of 5% TCA, and filtered over glass fiber filters (GF/C filters, Whatman). Filters were washed with 5% TCA, rinsed with ethanol, and dried. The radioactivity was quantitated by liquid scintillation counting (LSC). Enzyme activity was determined from plots of guanine incorporation versus time. Assays were conducted in replicate.

Kinetic Analyses. Steady-state kinetic parameters for the htTGT (wt) and the htTGT (D89E) mutant were determined at pH 7.3 and 8.5 using the guanine-exchange assay. Studies at pH 7.3 were performed in 100 mM HEPES as described above, while those at pH 8.5 were performed in a constant ionic strength buffer [100 mM 4-ethylmorpholine, 51 mM 2-(*N*-morpholino)ethanesulfonic acid, 51 mM diethanolamine] (*28*).

For the htTGT (wt), pH 7.3, the tRNA and guanine concentrations ranged from 0.075 to 10 μM. [8-^{3}H]Guanine (162 mCi/mmol) was used as the heterocyclic substrate. The enzyme concentration was 25 nM. For the htTGT (D89E) mutant, pH 7.3, the tRNA concentration ranged from 0.1 to 10 μM, and the guanine concentrations ranged from 0.1 to 20 μM. [8-^{14}C]Guanine (56.6 mCi/mmol) was used as the heterocyclic substrate. The enzyme concentration was 50 nM. In both cases, the total reaction volume was 400 μL.

Kinetic parameters at pH 8.5 were determined using [8-^{14}C]guanine (56.6 mCi/mmol) as the heterocyclic substrate. For htTGT (wt), the tRNA and guanine concentrations ranged from 0.075 to 10 μM. The final enzyme concentration was 25 nM in reaction mixture volumes of either 800 or 400 μL. For htTGT (D89E), the tRNA concentration ranged from 0.075 to 20 μM, and the guanine concentration ranged from 0.1 to 40 μM. The enzyme concentration was 50 nM in reaction volumes of either 800 or 400 μL.

Initial velocities (v_is) were obtained from linear regression of guanine incorporation versus time for various concentrations of both the tRNA substrate and the guanine substrate (while holding the other substrate at a constant, saturating concentration) and converted to reciprocal seconds by dividing by the enzyme concentration (25 or 50 nM) and the aliquot volume (150 or 70 μL). k_{cat} and K_m were determined by nonlinear regression analysis of plots of initial velocities (reciprocal seconds) versus substrate concentration.

Hydrolysis of 8-[^{14}C]Guanine from tRNA. To probe the ability of htTGT (wt) and htTGT (mutants) to catalyze the hydrolysis of guanine from position 34 of substrate tRNA in the absence of the heterocyclic base, "washout assays" were performed as follows. Enzyme (250 nM final concentration) was introduced to reaction mixtures (350 μL total volume) containing 10 mM HEPES (pH 7.3), 20 mM $MgCl_2$, 10 mM DTT, and 10 μM tRNA labeled with 8-[^{14}C]guanine at position 34. The reaction mixtures were incubated at 37 °C, and aliquots (50 μL) were withdrawn over a 3 h time course. As a control, duplicate reaction mixtures were prepared with the addition of 50 μM guanine and similarly assayed to ensure guanine "washout" could be observed. The aliquots were processed, and the radioactivity remaining in the tRNA was quantitated via LSC as described above. Hydrolytic activity was assessed by plots of guanine remaining versus time. Assays were performed in duplicate.

pH Dependence of the TGT Guanine Exchange Assay. The relationship between the pH of the reaction mixture and the enzyme activity was explored for all aspartate 89 mutants. Reaction conditions were similar to those used in the activity screen with the exceptions of pH and buffer system. pH values ranged from 7.3 to 9.0. HEPES buffer was used for the pH 7.3 reactions, while a previously described constant ionic strength buffer [100 mM 4-ethylmorpholine, 51 mM 2-(*N*-morpholino)ethanesulfonic acid, 51 mM diethanolamine] was used in the higher pH reactions (*28*). Enzyme

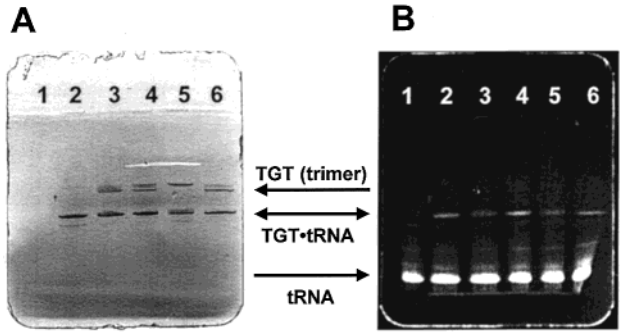

FIGURE 3: Native PAGE of tRNA binding to htTGTs. htTGT and D89 mutants (3 μM) were preincubated with tRNA (ECY, 30 μM) in a 10 μL reaction mixture containing 10 mM HEPES, pH 7.3, 1 mM $MgCl_2$, and 1 mM DTT at 37 °C for 1 h. Approximately 4 μL was loaded in each lane. Lanes: 1, tRNA alone; 2, htTGT (wt) + tRNA; 3, htTGT (D89A) + tRNA; 4, htTGT (D89C) + tRNA; 5, htTGT (D89E) + tRNA; 6, htTGT (D89N) + tRNA. (A) The gel was stained with Coomassie blue to visualize the protein-containing bands. (B) The gel was stained with ethidium bromide and photographed on a UV transilluminator to visualize tRNA-containing bands.

activity was monitored over a 4 h time course as described above. Enzyme activity at each pH was determined through linear regression of the plot of guanine incorporated versus time. Specific activities were obtained by dividing the slope of the plots by the TGT concentration (250 nM−2 μM) and the aliquot volume (70 μL). Assays were conducted in triplicate.

RESULTS

Construction, Overexpression, and Purification of the D89 Mutants. The desired glutamate (D89E), asparagine (D89N), cysteine (D89C), and alanine (D89A) mutations of position 89 were introduced into the *E. coli* TGT (wt) via site-directed mutagenesis of the *tgt* gene from the expression plasmid pTGT5 (*27*). The resulting mutant *tgt* genes were sequenced to confirm the presence of only the desired mutation.

From the resulting plasmids, mutant TGT expression was first attempted in the *tgt*$^-$ bacterial strain *E. coli* ΔK12(DE3) pLysS. Because it does not contain a chromosomal copy of the *tgt* gene, this *E. coli* strain is routinely used in our laboratory to generate mutants of the *E. coli* TGT. However, using this strain, only TGT (D89E) was successfully overexpressed.

Previous experience in our laboratory suggested that generation of the TGT mutants might be achieved by attaching an amino-terminal histidine tag and expressing in a *tgt*$^+$ bacterial strain (i.e., BL21). To append the 6-histidine-tag sequence to the mutant enzymes, each *tgt* mutant was excised from the corresponding pTGT5 plasmid via double restriction digestion (*Nde*I and *Hin*dIII) and ligated into a complementarily digested pET28a plasmid. Restriction enzyme digestions, as indicated in Table 1, were used to confirm the presence of each mutant *tgt* gene in pET28a. From the resulting plasmids, the four mutant TGTs were successfully overexpressed in the bacterial host BL21(DE3) pLysS. The wild-type TGT was also expressed with an appended amino-terminal His tag in the same bacterial strain. Each htTGT (mutants and wild type) was purified to homogeneity by nickel affinity chromatography (data not shown). Typical enzyme yields averaged between 12 and 16 mg of protein/L of cell culture.

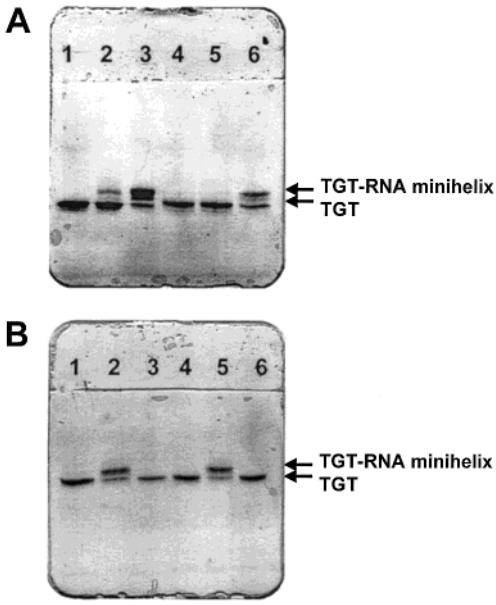

FIGURE 4: SDS−PAGE of the htTGT•tRNA stable complex. htTGT and D89 mutants (5 μM) were preincubated with tRNA (dG_{34}-ECYMH, 20 μM) in a 10 μL reaction mixture containing 10 mM HEPES, pH 7.3, 1 mM $MgCl_2$, and 1 mM DTT at 37 °C for 1 h. Following the addition of 10 μL of SDS buffer, reactions were incubated for an additional 1 h at room temperature. (A) Native TGT (wt) and htTGT (wt) with ECY and dG_{34}-ECYMH. Lanes: 1, native TGT (wt) alone; 2, native TGT (wt) + ECY; 3, native TGT (wt) + dG_{34}-ECYMH; 4, htTGT (wt) alone; 5, htTGT (wt) + ECY; 6, htTGT (wt) + dG_{34}-ECYMH. (B) htTGT (wt) and htTGT (mutants) complexed with dG_{34}-ECYMH. Lanes: 1, htTGT (wt) alone;2, htTGT (wt) + dG_{34}-ECYMH; 3, htTGT (D89A) + dG_{34}-ECYMH; 4, htTGT (D89C) + dG_{34}-ECYMH; 5, htTGT (D89E) + dG_{34}-ECYMH; 6, htTGT (D89N) + dG_{34}-ECYMH.

tRNA Binding to Wild-Type and Mutant TGTs. The ability of the htTGT (wt) and mutant htTGTs to bind substrate tRNA was assessed via native PAGE. Under native PAGE conditions, wild-type TGT migrates to an apparent M_r of ∼130000, consistent with a trimeric quaternary structure (*7*, *29*). When incubated with saturating levels of tRNA substrate, the TGT band shifts to an apparent M_r of ∼70000, which is consistent with a monomer TGT•tRNA complex. As shown in Figure 3A (lanes 2−6), the htTGT (wt) and the aspartate 89 mutants have bands corresponding to the TGT•tRNA complex. These bands all contain tRNA as evidenced by the coincidence of ethidium bromide staining (Figure 3B, comparing lanes 2−6 with lane 1).

Covalent Complex Band-Shift Assay. The presence of a stable TGT•tRNA complex has previously been observed under SDS−PAGE conditions (*15*). Although it has yet to be established that this complex represents a true enzyme−tRNA covalent intermediate, a correlation has been observed between the formation of this complex and enzymatic activity (*11*). Interestingly, the histidine-tagged wild-type TGT does not exhibit a covalent complex band with either full-length tRNA (data not shown) or the minihelical RNA, ECYMH (Figure 4A). Under mild denaturing conditions, both native TGT (wt) and htTGT (wt) demonstrate the ability to form this complex with the tRNA analogue, dG_{34}-CYMH, as evidenced by the observable 50 kDa band (Figure 4A). None of the htTGT mutants exhibited a covalent complex band with ECYMH (data not shown). However, htTGT (D89E) did exhibit this complex with dG_{34}-ECYMH (Figure 4B). It

Table 2: Specific Activities of His-Tagged TGTs at pH 7.3

	specific activity[a] (10^{-6} s^{-1})	relative specific activity
TGT (wt)[b]	2202 (30)	
htTGT (wt)	1290 (30)	1
htTGT (D89E)	570 (80)	0.44
htTGT (D89C)	8.9 (0.36)	0.0069
htTGT (D89N)	8.7 (2.1)	0.0067
htTGT (D89A)	6.2 (3.5)	0.0048

[a] Specific activities for the wild-type and D89E htTGTs were determined in triplicate at 50 nM enzyme and 20 μM substrate. The specific activities for the D89A, D89C, and D89N mutants were determined in triplicate at the following enzyme concentrations: 250 nM, 500 nM, 1 μM, and 2 μM. The values reported are the average of all determinations with the standard error in parentheses. [b] The specific activity for TGT (wt) is taken from Chong et al. (*43*).

appears that the histidine tag reduces the stability of the covalent complex with "normal" RNA substrates. The dG_{34}-containing minihelix is a substrate for TGT and has been noted to form a strong covalent complex (as evidenced by a larger degree of band shifting and a more intense shifted band) (*30*; Nonekowski and Garcia, unpublished). A manuscript is in preparation that fully describes this.

On the basis of experience in our laboratory, the observation of a covalent complex with htTGT (D89E) suggests that this mutant is active and the lack of complexes for the other mutants would indicate that they have dramatically impaired (or no) activity.

Activity Screen of the Aspartate 89 Mutants: Guanine-Exchange Assay. The htTGT mutant enzymes were assessed for their ability to catalyze the guanine-exchange reaction using saturating amounts of tRNA and [8-^{14}C]guanine substrates. In this assay, the htTGT (wt) demonstrated activity comparable to that of the native TGT (Table 2). This suggests that the presence of the amino-terminal histidine tag did not have a negative impact on enzyme catalysis. The htTGT (D89E) exhibited activity that was about 2-fold less than that of the htTGT (wt) (Table 2). Over a time course of 4 h, the htTGT (D89N), htTGT (D89C), and htTGT (D89A) also exhibited guanine-exchange capability. However, the activity of these enzymes was reduced by about 3 orders of magnitude compared to htTGT (wt) and htTGT (D89E) (Table 2). The observed activity for these three htTGT mutants was demonstrated to be linear with respect to enzyme concentrations ranging from 250 nM to 2 μM (data not shown). This is consistent with the covalent complex band-shift assay results above.

Kinetic Analysis of the His WT and Asp89 Mutants. Kinetic parameters for the htTGT (wt) and the htTGT (D89E) at pH 7.3 and 8.5 were determined by nonlinear fits to the Michaelis−Menten equation (Figure 5, Table 3). At pH 8.5, the htTGT (wt) exhibited a 5−6-fold increase in k_{cat} when compared to pH 7.3. In contrast, the increase in reaction pH had little effect on the k_{cat} of the htTGT (D89E). K_m values varied slightly between the two pH values, with the higher pH of 8.5 exhibiting increased K_m values for both enzymes.

At either pH, the most profound effect of the D89E mutation was observed in the K_m value for guanine, which was increased by a factor of 26 compared to the htTGT (wt) at pH 7.3 and by a factor of 11 at pH 8.5. Both enzymes exhibited similar K_m values for tRNA at either pH. The D89E mutation did not significantly affect the k_{cat} value at pH 7.3,

Table 3: Kinetic Parameters for htTGT (wt) and htTGT (D89E) at pH 7.3 and 8.5

	K_m[a] (μM)	k_{cat}[a] (10^{-3} s^{-1})	k_{cat}/K_m[a] (10^{-3} s^{-1} μM^{-1})	rel k_{cat}/K_m (10^{-3} s^{-1} μM^{-1})	rel k_{cat} (10^{-3} s^{-1})
tRNA and Guanine Kinetics at pH 7.3					
tRNA					
htTGT (wt)	0.12 (0.04)	1.21 (0.07)	10.1 (3.4)	1	1
htTGT (D89E)	0.11 (0.03)	0.71 (0.03)	6.45 (1.78)	0.64	0.59
guanine					
htTGT (wt)	0.10 (0.03)	1.21 (0.07)	12.1 (3.7)	1	1
htTGT (D89E)	2.61 (0.33)	0.59 (0.02)	0.23 (0.03)	0.02	0.49
tRNA and Guanine Kinetics at pH 8.5					
tRNA					
htTGT (wt)	0.39 (0.07)	5.85 (0.29)	15.0 (2.8)	1	1
htTGT (D89E)	0.51 (0.14)	0.93 (0.06)	1.82 (0.51)	0.12	0.16
guanine					
htTGT (wt)	0.57 (0.05)	7.57 (0.17)	13.3 (1.2)	1	1
htTGT (D89E)	6.32 (1.41)	0.75 (0.05)	0.12 (0.03)	0.009	0.09

[a] Standard errors are in parentheses.

which was only decreased by about a factor of 2 compared to the htTGT (wt). As a result, the catalytic efficiency (as defined by k_{cat}/K_m) was decreased by ca. 50-fold for guanine but only 2-fold for tRNA at pH 7.3. However, at pH 8.5, the k_{cat} of the htTGT (D89E) was reduced by a factor of ca. 10-fold compared to htTGT (wt). Coupled with the slight increase in K_m values at pH 8.5, the catalytic efficiency of htTGT (D89E) was decreased 100-fold for guanine and 10-fold for tRNA.

Due to their low degree of activity, even under normally saturating substrate conditions, it was not feasible to perform detailed kinetic analyses on the htTGT (D89N), htTGT (D89C), and htTGT (D89A) enzymes.

pH Studies of the Aspartate 89 Mutants. The relationship between specific activity and reaction pH was explored for htTGT (D89E), htTGT (D89N), htTGT (D89C), and htTGT (D89A). The specific activity of each mutant was measured at pH 7.3, 8.0, 8.5, and 9.0. On the basis of results shown in Figure 6A, it is apparent that the activities of htTGT (D89A), htTGT (D89C), and htTGT (D89N) are optimal around pH 8.5. Furthermore, the observed pattern of pH dependence versus activity appears to be very similar in all three cases. Similar pH dependencies are also observed for htTGT (D89E) (Figure 6B) and htTGT (wt) (Figure 6C).

Hydrolysis of 8-[^{14}C]Guanine from tRNA. htTGT (D89A), htTGT (D89C), and htTGT (D89N) were investigated for their ability to act as G_{34}-specific hydrolases using a washout assay. In this assay, the "deguanylation" of substrate tRNA by each htTGT was probed in the absence of heterocyclic substrate. Over a 3 h time course, no G_{34} hydrolysis was observed with any of the mutant htTGTs. In comparison, radiolabel washout was observed with htTGT (wt) in the presence of both [8-^{14}C]guanine$_{34}$-labeled tRNA and saturating guanine.

DISCUSSION

Previously, Romier et al. have proposed a double displacement mechanism for catalysis by TGT that is characterized by the formation of a covalent enzyme−ribosyl (tRNA) intermediate (*14*). On the basis of its position in the crystal structure of the *Z. mobilis* enzyme, aspartate 102 (aspartate

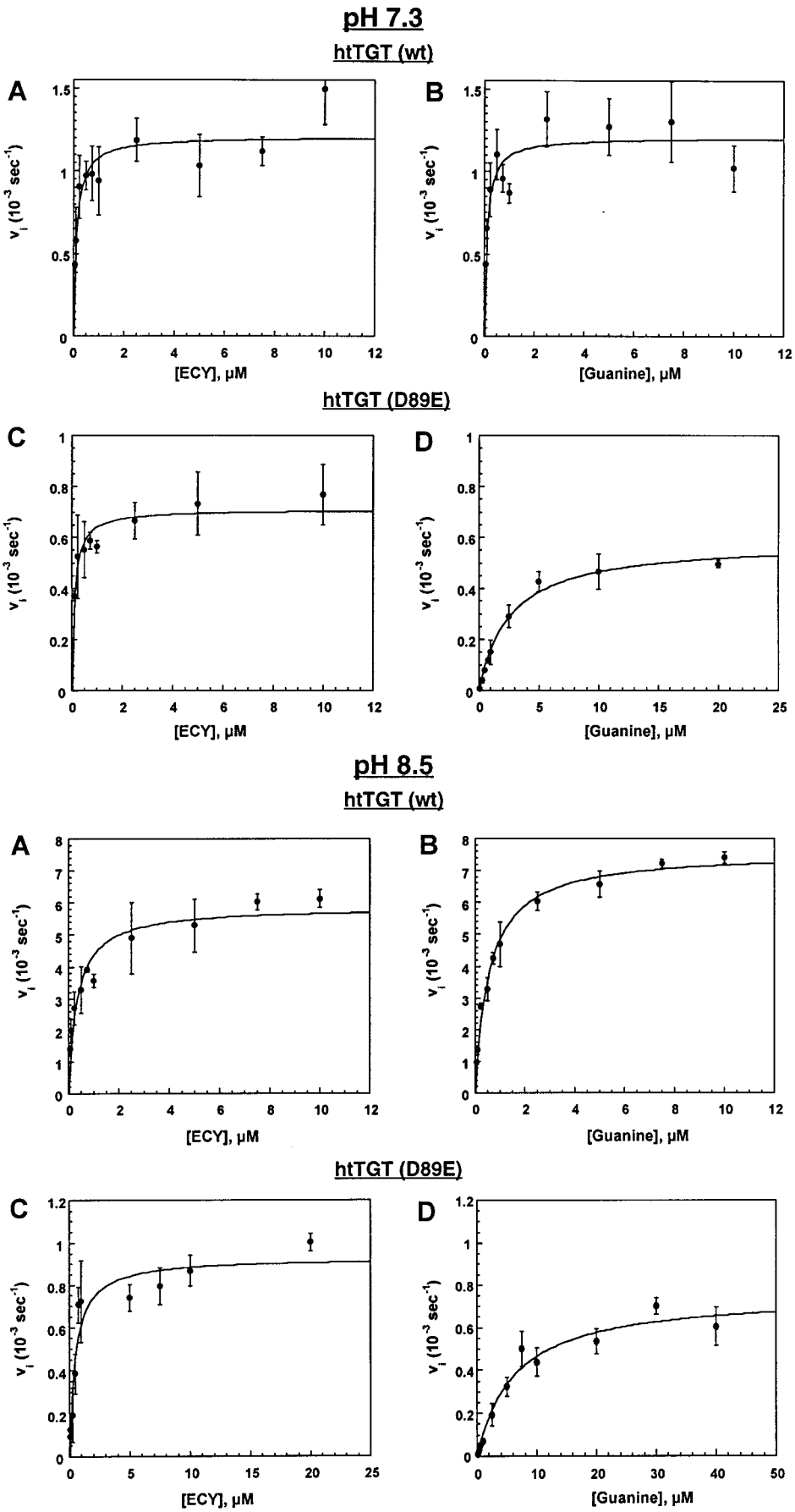

FIGURE 5: Michaelis−Menten plots of htTGT (wt) and htTGT (D89E) at pH 7.3 and 8.5. The averages of data points obtained from three independent determinations are plotted. The curves represent fits of the data calculated by nonlinear regression. Error bars were generated from the standard deviation within each point. Panels: (A) htTGT (wt) tRNA (ECY) kinetics; (B) htTGT (wt) guanine kinetics; (C) htTGT (D89E) tRNA (ECY) kinetics; (D) htTGT (D89E) guanine kinetics.

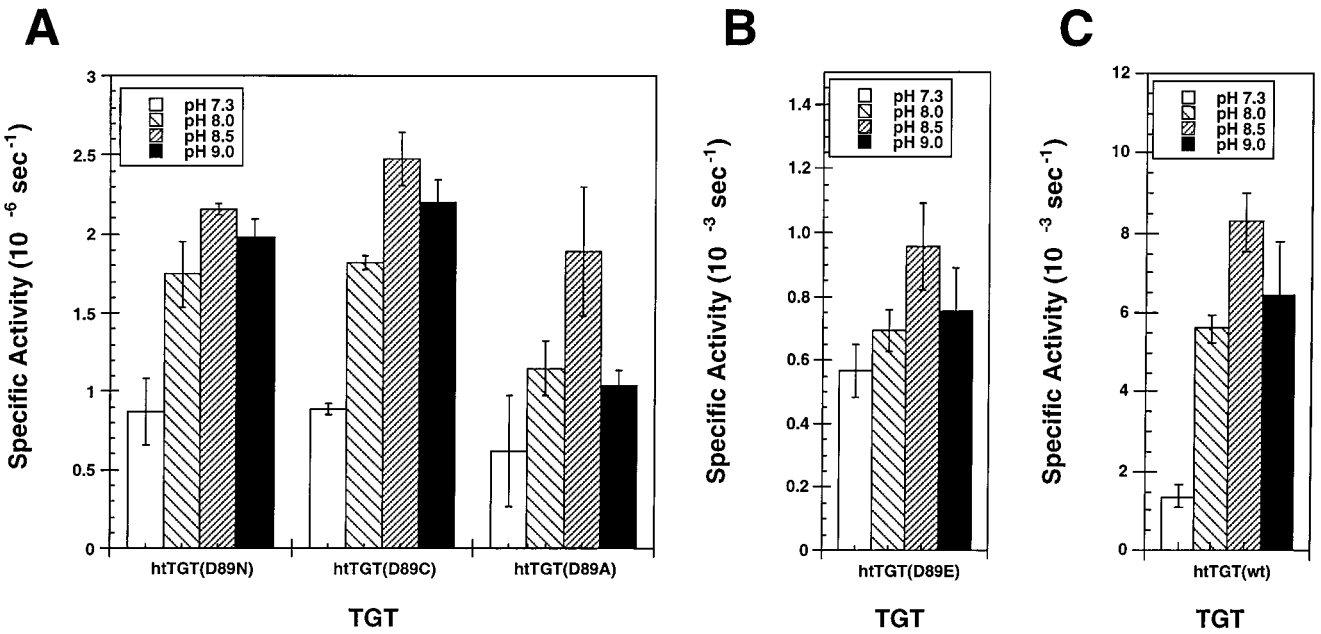

FIGURE 6: pH dependence of htTGT specific activities. Enzyme activity at each pH was determined through linear regression of a 4 h time course of guanine incorporation versus time as described in Materials and Methods. Specific activities were obtained by dividing the slope of the plots by the enzyme concentration (250 nM−2 μM) and the aliquot volume (70 μL). Error bars are the standard deviation of triplicate determinations. Panels: (A) htTGT (D89A), htTGT (D89C), htTGT (D89N); (B) htTGT (D89E); (C) htTGT (wt).

89, *E. coli* numbering) was implicated as the potential enzymic nucleophile that is involved in the formation of this intermediate (*14*, *15*). Evidence for a TGT·tRNA covalent complex was provided by the observation of an approximately 70 kDa band on SDS−PAGE under mild denaturing conditions. Furthermore, an alanine mutant of this aspartate was shown to be inactive and unable to form the TGT·tRNA covalent intermediate complex, thereby demonstrating the importance of aspartate 102 in the catalytic mechanism of TGT.

Although this evidence is consistent with nucleophilic catalysis by aspartate 102, a dissociative type mechanism in which aspartate 102 acts to stabilize an oxocarbenium ion intermediate on the normal reaction pathway cannot be dismissed. This type of mechanistic intermediate has previously been demonstrated for other enzymes that are involved in the scission of C−N glycosidic bonds. Examples include the nucleoside hydrolases (*25*, *26*, *31*−*33*). It should be pointed out that the observation of the TGT·tRNA covalent intermediate would not be inconsistent with this mechanism. The covalent intermediate is observed only when the enzyme is incubated with a large excess of tRNA for relatively long time periods. Under these conditions, it is certainly possible that the aspartate could covalently trap the oxocarbenium intermediate. In our laboratory, we have observed a higher degree of covalent adduct formation with minihelical RNAs (*11*). However, these minihelical RNAs serve as poorer substrates (e.g., lower k_{cat}) in the TGT reaction when compared to their full-length counterparts. These observations are consistent with the idea that a longer lived oxocarbenium ion (that may occur if it is involved in the reduction in k_{cat}) would be trapped more efficiently by the aspartate residue.

To determine if catalysis by TGT occurs via an associative or dissociative mechanism, we have generated four different mutations of aspartate 89 in the *E. coli* TGT: asparagine, cysteine, glutamate, and alanine. These mutants were constructed with an appended histidine tag (six histidines) at the amino terminus. The histidine tag was included in order to be able to efficiently separate the mutant enzymes from any host-derived wild-type TGT. It should be noted that the amino terminus of TGT is on the opposite side of the enzyme from the active site; therefore, the His tag is not expected to affect activity. We have generated the wild-type TGT with the appended histidine tag and confirmed that its activity is comparable to that of the wild-type enzyme (Abold and Garcia, unpublished). All four aspartate 89 TGT mutants exhibited similar expression and purification behavior (data reviewed but not shown). Furthermore, each aspartate 89 mutant TGT was able to bind substrate tRNA, thereby ruling out the possibility that the mutations resulted in a change of the gross conformation of the enzyme (Figure 3).

The htTGT (D89E) mutant exhibited levels of activity that were just slightly lower than those of the htTGT (wt) at pH 7.3, the pH at which TGT has predominantly been assayed. However, at pH 8.5, the two enzymes displayed a larger difference in activity. Kinetic parameters determined at both pH 7.3 and pH 8.5 (Figure 5 and Table 3) reveal that the k_{cat} of htTGT (wt) at pH 8.5 was greater than at pH 7.3. In contrast, the k_{cat} of htTGT (D89E) varied only slightly between the two pHs. Aside from the differences in catalysis, the htTGT (D89E) also demonstrated an increase in K_m for guanine. The significant differences in activity between htTGT(wt) and htTGT (D89E) suggest that the glutamate is not optimally positioned for catalysis, consistent with the models in Figure 7. On the surface, the level of activity of the D89E mutant appears to be consistent with either mechanism. However, Muraki et al. (*34*) found that a glutamate mutant of aspartate 53 in human lysozyme exhibited a similar activity reduction relative to wild type and concluded that a nucleophilic mechanism was at least partly involved in catalysis. The activity of the htTGT (D89E) mutant reveals a considerable tolerance for the positioning of the carboxylate in the TGT active site.

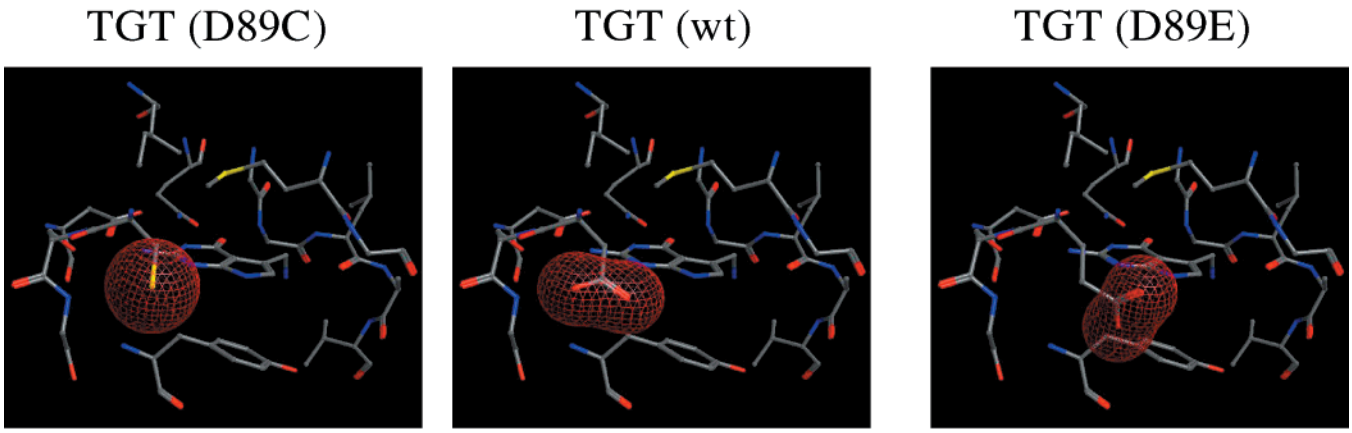

FIGURE 7: Active site of the *Z. mobilis* TGT: wild type versus models of cysteine and glutamate mutants of aspartate 89. Models of the *Z. mobilis* TGT active site containing preQ$_1$ were generated from coordinates provided by Dr. Ralf Ficner. The cysteine (as the thiolate) and glutamate mutants of aspartate 89 were made and displayed using MOE (Molecular Operating Environment, Chemical Computing Group Inc.) on a SGI Octane 2 workstation. The orientations of the cysteine and glutamate side chains were adjusted to remove any steric conflicts.

The htTGT (D89N), htTGT (D89C), and htTGT (D89A) mutant enzymes exhibited very low levels of guanine exchange activity. Theses activities, observed over a 4 h time course, were linear with respect to enzyme concentrations ranging from 250 nM to 2 μM. However, the activity of each mutant is roughly 3 orders of magnitude lower than that observed with wild-type enzyme and the D89E mutant. Considering this, it seems unlikely that an oxocarbenium ion transition state occurs in the normal TGT reaction pathway. Nonetheless, the fact that any activity was observed for these three mutants warranted further investigation. Two possibilities that might account for the observed activity of the htTGT (D89N), htTGT (D89C), and htTGT (D89A) enzymes were considered. First, it is possible that the observed activity is intrinsic to each of these enzymes. Although the corresponding D102A mutant in *Z. mobilis* was found to be inactive (*15*), it was not reported if the experiments probed for very low level (ca. 10^3-fold lower than wild type) activity. It is possible that a water molecule could substitute for the aspartate 89 carboxylate, resulting in a very reduced activity. It is also possible that these mutants may have an altered chemical mechanism that is more like the dissociative mechanism in Figure 2; however, this is not consistent with the observed pH profile for the cysteine mutant (discussed below).

Second, the more likely possibility is that the observed activities of the htTGT (D89A), htTGT (D89C), and htTGT (D89N) mutants are the result of contamination due to chromosomally derived TGT (wt) from the bacterial host. As mentioned previously, each of the aspartate 89 mutants was constructed with an amino-terminal histidine tag in order to provide a means to separate them from any host-generated wild type. It is important to note that studies performed in our laboratory have demonstrated that the wild-type recombinant TGT exhibits a trimeric quaternary structure that dissociates into a monomeric form upon tRNA binding (*7*, *29*). It is unclear if the trimeric structure is realized in vivo. Nonetheless, it is possible that the observed activity of the htTGT (D89N), htTGT (D89C), and htTGT (D89A) mutants could be the result of chromosomally derived wild-type monomers that have been integrated into the trimeric structure of the mutant TGTs, essentially forming a heterotrimer. It seems plausible that the purification properties of the heterotrimer would not differ much from the homotrimeric mutant since each heterotrimer would contain at least one histidine-tag sequence.

Interestingly, of the four mutant TGTs studied, only the D89E could be expressed in a *tgt*$^-$ bacterial strain. While the significance of this is unclear, it was intriguing to hypothesize that perhaps the D89A, D89C, and D89N mutants might act as G_{34}-tRNA specific hydrolases, thereby displacing G_{34} from cognate tRNA species in vivo. Given this, expression of the mutant TGTs would be expected to have a direct negative impact on protein translation by disrupting the anticodon sequence of queuine-cognate tRNAs. However, we did not observe any in vitro G_{34} hydrolytic activity in the absence of guanine over a 3 h time course.

A detailed analysis of the kinetic parameters for the htTGT (D89N), htTGT (D89C), and htTGT (D89A) would be useful in determining if wild-type TGT contamination were the source of the activity. Unfortunately, the activities observed with each of these mutant enzymes were too low to accurately determine the K_m values. The dependence of specific activity upon pH was similar for all three mutants as well as wild type and htTGT (D89E) although at much higher levels of activity, with pH 8.5 being the optimum in all three cases (Figure 6). Furthermore, we have observed variations in specific activity from different preparations of these three TGT mutants. (Three independent preparations of each of the low-activity mutants were assayed at the pH optimum of 8.5. The specific activities varied by factors of 2−5-fold while the standard deviations within the determinations were 10−20%.) This is consistent with the activities of these mutants being due to wild-type TGT contamination that varies somewhat from preparation to preparation. The observation that htTGT (D89C) has a pH profile similar to that of the other mutants and wild-type TGT suggests that deprotonation of the cysteine thiol has little effect on catalysis. This is again consistent with the associative mechanism, where a cysteine thiolate would not be able to substitute for the aspartate 89 carboxylate. Although the cysteine side chain does possess nucleophilic character, mutagenic studies of retaining β-glycohydrolases suggest that it cannot assume the role of a nucleophilic glutamate (*35*). However, it is not unreasonable to believe that the thiolate anion of a cysteine residue could serve to stabilize an

oxocarbenium ion. If catalysis by TGT were to proceed through a dissociative mechanism, it is likely that cysteine stabilization of an oxocarbenium ion intermediate would be most efficient at higher pH where the cysteine would be in the thiolate form. This suggests that the D89C mutant should have a pH−activity profile that is significantly different from the wild type and other mutants if the dissociative mechanism is operative, which was not observed. One caveat to our conclusion is that the pK_a of the cysteine thiol could be perturbed in the active site to a value higher than the highest pH studied (9.0). Attempts to probe cysteine pK_as in TGT via spectrophotometric and other means have been confounded by the fact that the wild-type *E. coli* TGT contains eight cysteines (Goodenough-Lashua and Garcia, unpublished).

If the TGT reaction pathway proceeds via electrostatic stabilization by aspartate 89 in a dissociative mechanism, then the D89E and the D89N mutants should exhibit significant levels of activity. Glutamate is an obvious isoelectronic replacement of aspartate. Asparagine is an isosteric replacement, and while it would not be expected to stabilize the positive charge associated with the oxocarbenium ion as well as the carboxylate of aspartate, owing to the electron density in the amide group of asparagine, some stabilization could conceivably occur. Alternatively, if aspartate 89 serves as a nucleophile in an associative mechanism, it is still likely that the conservative glutamate mutation would retain a significant level of activity. Glutamate has been identified as the catalytic nucleophile in a number of glycosidases (*18*−*21*). However, the D89N mutant would not be expected to be catalytically competent in this mechanism. Amides have been noted to act as nucleophiles through the amide oxygen, but this has been seen only with very activated electrophiles and in highly oriented systems (*36*−*38*). In only one case that we are aware of has an asparagine been observed to act nucleophilically in an enzymic reaction, through a cyanoalanine intermediate (*39*). An asparagine mutant of the catalytic nucleophile aspartate in haloalkane dehalogenase has been found to be inactive but can be activated by deamidation back to aspartate (*40*). Recently, it has been reported that catalysis by hen egg white lysozyme actually proceeds via a covalent mechanism involving aspartate 52 (*41*). While Kirsch and co-workers found that an asparagine mutant of this aspartate exhibited a significant level (ca. 5%) of activity (*42*), that activity was attributed to chemical rescue by carboxylate groups in the cell wall substrate that was used and not to the asparagine mutation. Although there are some exceptions in the literature, it is generally accepted that asparagines are very rarely found to be efficient enzymic nucleophiles but more often are able to support an oxocarbenium ion intermediate. We find that only htTGT (wt) and htTGT (D89E) demonstrated the ability to form a covalent complex with tRNA (Figure 4). Although this observation is not sufficient to prove the associative mechanism (as argued above), it does prove that a covalent complex can be formed and is consistent with an associative mechanism.

Steric models of the glutamate and cysteine mutations of the catalytic aspartate were generated from the crystal coordinates of the *Z. mobilis* TGT complexed with its preQ$_1$ substrate (Figure 7). It appears that these changes do not dramatically disrupt the TGT active site, as both of the mutant side chains generally occupy similar positions relative to the native aspartate. The sulfur, modeled as the thiolate, of the cysteine mutant occupies virtually the same position as the carboxylate of the wild-type aspartate, suggesting that the position of the thiolate should not impair its ability to stabilize an oxocarbenium ion intermediate. It is apparent that the carboxylate moiety of the glutamate side chain is oriented differently when compared to that of the aspartate side chain. However, this model and the crystal structure it is derived from do not include the tRNA substrate. Therefore, it is impossible to predict with any certainty how this difference in placement of the carboxylate would affect enzymatic activity.

The very low levels of activity exhibited by the alanine, asparagine, and cysteine mutants strongly suggest that the dissociative mechanism is not utilized by TGT. The pH studies and the variant activities of the replicate enzyme preparations are consistent with this low activity being due to very small (ca. 0.1%) contamination by TGT (wt). This, combined with the near-wild-type activity of the htTGT (D89E) mutant, is most consistent with an associative mechanism for TGT and a nucleophilic role for aspartate 89.

ACKNOWLEDGMENT

We gratefully acknowledge the technical assistance of Elisa Babilonia-Babilonia in preparing plasmids pD89A, pD89E, and pD89N. We thank Dr. Ralf Ficner for providing the coordinates of the *Z. mobilis* TGT·preQ$_1$ complex. We also thank Ms. Katherine Abold and Dr. Heather Carlson for generating the computer models and for the preparation of Figure 7. Finally, we thank members of our laboratory for critical reviews of the manuscript and helpful discussions.

REFERENCES

1. Slany, R. K., Bosl, M., and Kersten, H. (1994) *Biochimie 76*, 389−393.
2. Frey, B., McCloskey, J., Kersten, W., and Kersten, H. (1988) *J. Bacteriol. 170*, 2078−2082.
3. Kasai, H., Nakanishi, K., Macfarlane, R. D., Torgerson, D. F., Ohashi, Z., McCloskey, J. A., Gross, H. J., and Nishimura, S. (1976) *J. Am. Chem. Soc. 98*, 5044.
4. Watanabe, M., Matsuo, M., Tanaka, S., Akimoto, H., Asahi, S., Nishimura, S., Katze, J. R., Hashizume, T., Crain, P. F., McCloskey, J. A., and Okada, N. (1997) *J. Biol. Chem. 272*, 20146−20151.
5. Bai, Y., Fox, D. T., Lacy, J. A., Van Lanen, S. G., and Iwata-Reuyl, D. (2000) *J. Biol. Chem. 275*, 28731−28738.
6. Curnow, A. W., Kung, F. L., Koch, K. A., and Garcia, G. A. (1993) *Biochemistry 32*, 5239−5246.
7. Curnow, A. W., and Garcia, G. A. (1994) *Biochimie 76*, 1183−1191.
8. Curnow, A. W., and Garcia, G. A. (1995) *J. Biol. Chem. 270*, 17264−17267.
9. Nakanishi, S., Ueda, T., Hori, H., Yamazaki, N., Okada, N., and Watanabe, K. (1994) *J. Biol. Chem. 269*, 32221−32225.
10. Kung, F.-L., and Garcia, G. A. (1998) *FEBS Lett. 431*, 427−432.
11. Kung, F. L., Nonekowski, S., and Garcia, G. A. (2000) *RNA 6*, 233−244.
12. Hoops, G. C., Townsend, L. B., and Garcia, G. A. (1995) *Biochemistry 34*, 15381−15387.
13. Romier, C., Ficner, R., Reuter, K., and Suck, D. (1996) *Proteins: Struct., Funct., Genet. 24*, 516−519.

14. Romier, C., Reuter, K., Suck, D., and Ficner, R. (1996) *EMBO J. 15*, 2850−2857.
15. Romier, C., Reuter, K., Suck, D., and Ficner, R. (1996) *Biochemistry 35*, 15734−15739.
16. Porter, D. J. T., Merrill, B. M., and Short, S. A. (1995) *J. Biol. Chem. 270*, 15551−15556.
17. Porter, D. J. T., and Short, S. A. (1995) *J. Biol. Chem. 270*, 15557−15562.
18. Miao, S., Ziser, L., Aebersold, R., and Withers, S. G. (1994) *Biochemistry 33*, 7029/7032.
19. Zechel, D. L., He, S., Dupont, C., and Withers, S. G. (1998) *Biochem. J. 336*, 139−145.
20. Wong, A. W., He, S., Grubb, J. H., Sly, W. S., and Withers, S. G. (1998) *J. Biol. Chem. 273*, 34057−34062.
21. Vocadlo, D. J., MacKenzie, L. F., He, S., Zeikus, G. J., and Withers, S. G. (1998) *Biochem. J. 335*, 449−455.
22. McCarter, J. D., and Withers, S. G. (1996) *J. Biol. Chem. 271*, 6889−6894.
23. Vocadlo, D. J., Mayer, C., He, S. M., and Withers, S. G. (2000) *Biochemistry 39*, 117−126.
24. Huang, L. X., Pookanjanatavip, M., Gu, X. G., and Santi, D. V. (1998) *Biochemistry 37*, 344−351.
25. Degano, M., Almo, S. C., Sacchettini, J. C., and Schramm, V. L. (1998) *Biochemistry 37*, 6277−6285.
26. Horenstein, B. A., Parkin, D. W., Estupinan, B., and Schramm, V. L. (1991) *Biochemistry 30*, 10788−10795.
27. Chong, S., and Garcia, G. A. (1994) *BioTechniques 17*, 686−691.
28. Ellis, K. J., and Morrison, J. F. (1982) *Methods Enzymol. 87*, 405−426.
29. Reuter, K., Chong, S., Ullrich, F., Kersten, H., and Garcia, G. A. (1994) *Biochemistry 33*, 7041−7046.
30. Kung, F.-L. (1998), Ph.D. Thesis, University of Michigan, Ann Arbor.
31. Dewolf, W. E., Emig, F. A., and Schramm, V. L. (1986) *Biochemistry 25*, 4132−4140.
32. Mentch, F., Parkin, D. W., and Schramm, V. L. (1987) *Biochemistry 26*, 921−930.
33. Parkin, D. W., and Schramm, V. L. (1987) *Biochemistry 26*, 913−920.
34. Muraki, M., Harata, K., Hayashi, Y., Machida, M., and Jigami, Y. (1991) *Biochim. Biophys. Acta 1079*, 229−237.
35. Lawson, S. L., Warren, R. A. J., and Withers, S. G. (1998) *Biochem. J. 330*, 203−209.
36. Knapp, S., Vocadlo, D., Gao, Z., Kirk, B., Lou, J., and Withers, S. G. (1996) *J. Am. Chem. Soc. 118*, 6804−6805.
37. Drouillard, S., Armand, S., Davies, G. J., Vorgias, C. E., and Henrissat, B. (1997) *Biochem. J. 328*, 945−949.
38. Mark, B. L., Vocadlo, D. J., Knapp, S., Triggs-Raine, B. L., Withers, S. G., and James, M. N. (2001) *J. Biol. Chem. 276*, 10330−10337.
39. Ichiyama, S., Kurihara, T., Li, Y. F., Kogure, Y., Tsunasawa, S., and Esaki, N. (2000) *J. Biol. Chem. 275*, 40804−40809.
40. Pries, F., Kingma, J., and Janssen, D. B. (1995) *FEBS Lett. 358*, 171−174.
41. Vocadlo, D., Davies, G., Laine, R., and Withers, S. (2001) *Nature (London) 412*, 835−838.
42. Malcolm, B. A., Rosenberg, S., Corey, M. J., Allen, J. S., de Baetselier, A., and Kirsch, J. F. (1989) *Proc. Natl. Acad. Sci. U.S.A. 86*, 133−137.
43. Chong, S., Curnow, A. W., Huston, T. J., and Garcia, G. A. (1995) *Biochemistry 34*, 3694−3701.

BI0110589